Low-ozone events in the southern polar summer as indicated by Met Office ozone analyses

D. R. Jackson,[1] Y. J. Orsolini,[2] and O. Engelsen[2]

Received 4 August 2010; revised 21 December 2010; accepted 11 January 2011; published 17 March 2011.

[1] Southern summer low-ozone events (LOEs) are examined using Met Office ozone analyses for 2005–2007. At 31 hPa, tongues of low-ozone air are pulled out of the polar region and extend to lower latitudes. Low tongues are also seen at 100 hPa, but there the low ozone is transported from low to high latitudes. These low tongues are frequently superimposed on one another, meaning that there are often also reductions in total ozone. What is striking is that at high latitudes, summer total ozone is typically lower over the Weddell Sea than at other longitudes. The low-ozone tongues at 31 and 100 hPa are consistent with transport associated with planetary waves. Daily geopotential height fields show a poleward and westward wave tilt with height, indicating the presence of baroclinic waves. The tilt enables the superimposition of the low-ozone tongues at 100 and 31 hPa. Filtered geopotential height anomalies reveal the presence of waves reported in other studies and indicate the connection between tropospheric and stratospheric wave dynamics in driving the LOEs. There is also a high connection between the LOEs and ultraviolet (UV) Index. The Weddell Sea region gets up to 20–30% more UV than the zonal mean, and the tip of South America gets about 10–25% more. There have been numerous studies of the impacts of increased UV on the Antarctic marine ecosystem during the springtime ozone hole, and our results indicate there is a case for these studies being extended to the summer LOEs.

Citation: Jackson, D. R., Y. J. Orsolini, and O. Engelsen (2011), Low-ozone events in the southern polar summer as indicated by Met Office ozone analyses, *J. Geophys. Res.*, *116*, D06302, doi:10.1029/2010JD014858.

1. Introduction

[2] It is well known that column total ozone levels undergo fluctuations in both hemispheres in winter and spring associated with the passage of tropospheric weather systems. Cases where rapid ozone reduction occurs are often referred to as "ozone miniholes" or "low ozone episodes" (LOE), and have been documented by a number of authors [e.g., *McKenna et al.*, 1989; *Newman et al.*, 1988; *Peters et al.*, 1995; *James*, 1998]. An ozone column reduction results from the presence of an anticyclone in the upper troposphere/lower stratosphere (UTLS). The associated raising of the tropopause means that a greater proportion of the column is occupied by ozone-poor tropospheric air. In addition, the divergence of ozone-rich air out of the column in the lower stratosphere leads to a further reduction in total ozone. The total ozone decrease comes from a combination of these motions plus the horizontal transport of ozone poor air from lower latitudes. The detailed dynamics is elucidated in a number of studies, including *Allen and Nakamura* [2002] and *Hood et al.* [2001, and references therein].

[3] Miniholes of moderate strength occur frequently in middle and high latitudes [*James*, 1998; *Orsolini et al.*, 1998], and a smaller number of very intense miniholes are often observed in combination with a sudden stratospheric warming or other distortion of the stratospheric polar vortex. Case studies of such events include those by *Allen and Nakamura* [2002], *Hood et al.* [2001], *Petzoldt et al.* [1994], *Petzoldt* [1999] and *Keil et al.* [2007]. In these events the horizontal advection of ozone-poor air present in the stratospheric polar vortex over a region where the ozone column is already reduced due to the presence of a UTLS anticyclone leads to an even larger reduction in the total ozone column. Low-ozone episodes have also been observed to develop over South America southern tip in the spring, and anticyclonic perturbations were shown to act as "seeds" to advect poleward tongues of ozone [*Canziani et al.*, 2002].

[4] The above case studies focused on the winter and spring, but LOEs also exist in summer. *Orsolini et al.* [2003] documented LOEs in the northern summer high latitudes. In the polar stratosphere, summertime ozone loss is dominated by nitrogen and hydrogen gas-phase catalytic cycles, which are efficient at high latitudes because of the long insolation. These chemical conditions, combined with relatively quiet dynamical conditions, allow a low-ozone pool of air to form over the pole. After formation, this low ozone can be transported to lower latitudes by planetary wave activity. Note that the upward propagation of planetary waves in the

[1]Met Office, Exeter, UK.
[2]Norwegian Institute for Air Research, Kjeller, Norway.

0148-0227/11/2010JD014858

lower and middle stratosphere is constrained by the location of the zero wind line, which is the critical level for quasi-stationary planetary waves.

[5] In the Southern Hemisphere summer, the lower stratospheric circulation is characterized by medium-scale quasi-stationary waves (wave numbers 4–6), first identified by *Schoeberl and Krueger* [1983], *Randel and Stanford* [1985], and further discussed by *Cariolle and Deque* [1986]. LOEs can occur from transport processes in the tropopause region, i.e., poleward transport of ozone-poor air and elevated tropopause in anticyclonic conditions, and be reinforced by transport aloft in the midstratosphere (i.e., the 20–30 km layer) when ozone from the Antarctic pool of low ozone is transported away from the pole toward lower latitudes. Such a LOE in February 2005 was first reported by *Jackson* [2007], in part of a broader study that focused on the assimilation of ozone data from the Earth Observing System Microwave Limb Sounder (EOS MLS) and the Solar Backscatter Ultraviolet Radiometer 2 (SBUV/2) instruments.

[6] Such summertime LOEs can lead to enhancements in surface ultraviolet (UV) radiation. However, previous studies of Southern Hemisphere ozone have usually focused on the spring. It has been shown in several papers [e.g., *Kirchhoff et al.*, 1997; *Pérez et al.*, 2000; *Cede et al.*, 2002; *Pazmiño et al.*, 2005, 2008; *de Laat et al.*, 2010], that the subpolar regions of the Southern Hemisphere are affected by short periods of low total ozone values directly linked to overpasses of the ozone hole. During these episodes, the subpolar regions experience a pronounced ozone reduction with generally an enhancement of UV-B radiation, depending on cloud cover conditions. Other studies have shown that the populated regions of the South America southern tip are a preferential area for vortex occurrences in the spring period [*Compagnucci et al.*, 2001; *Huth and Canziani*, 2003]. For example, *Pazmiño et al.* [2005] showed episodic daily erythemal dose increases larger than twice the climatological value at Ushuaia (54.9°S, 68.3°W) linked to vortex occurrences over the station during the period 1997–2003. The average erythemal UV increase due to these events was evaluated as 68% over this period.

[7] In this paper, the investigation of southern summer LOEs introduced by *Jackson* [2007] is extended. The synoptic evolution of the LOEs is described in more detail, and a dynamical explanation is attempted. In addition, while *Jackson* [2007] focused on January and February 2005, here the study is extended to the summers of 2005/2006 and 2006/2007.

[8] The layout of this paper is as follows. Details of the ozone and UV observations used in this study, and a summary of the data assimilation method appear in section 2. Section 3 contains a description of the LOEs seen in summer 2005 together with a discussion of the role of dynamics in their formation. LOEs seen in 2006 and 2007 are described in section 4, and in section 5 the impact of the LOEs on UV radiation is described. Conclusions are in section 6.

2. Data and Analysis Methods Used

2.1. Ozone Observations Assimilated

[9] In the experiments discussed here, ozone observations from EOS MLS and SBUV/2 are assimilated.

[10] Vn 1.51 EOS MLS retrievals are used for the 2005 and 2006 experiments, and vn 2.2 for the 2007 experiment. This was done because the 2005 and 2006 experiments were run when only vn 1.51 data were available, and the experiments are expensive and time consuming to rerun with vn 2.2 data. An assessment of the EOS MLS ozone profiles carried out by *Froidevaux et al.* [2008], showed that, compared to vn 1.51 retrievals, the vn 2.2 retrievals are in better agreement with correlative measurements, and in particular the error in the vertical gradient of stratospheric ozone (which led to positive biases in the lower stratosphere and negative biases in the upper stratosphere) is reduced. These differences are unlikely to have much impact on the comparison of results from 2005–2007 here, since a large focus is on horizontal spatial patterns in the ozone fields, and no horizontal variation in retrieval error for either version has been reported.

[11] The vertical resolution of the EOS MLS ozone profiles is ~3 km in the upper troposphere/lower stratosphere, degrading to ~4 km at 215 hPa and 6 km in the mesosphere. The profiles are considered to be useful in the 215–0.46 hPa range. *Froidevaux et al.* [2008] reported that the retrievals have an overall accuracy of ~1% in the stratosphere and typically less than ~10% in the upper troposphere (although sometimes the accuracy is 30–40% in the 200–300 hPa range). Comparison with other satellite data shows that in the stratosphere agreement is generally within 5–10% with data from the Halogen Occultation Experiment (HALOE), the Stratospheric Aerosol and Gas Experiment (SAGE II), the Polar Ozone and Aerosol Measurement (POAM III) and the Atmospheric Chemistry Experiment–Fourier Transform Spectrometer (ACE-FTS) (the versions of the HALOE, SAGE II, POAM III and ACE-FTS retrievals used in the comparison were vn 19, vn 6.2, vn 4 and vn 2.2 "ozone upgrade," respectively). The bias with respect to these data sets tends to be slightly too high in the lower stratosphere and slightly too low in the upper stratosphere. *Froidevaux et al.* [2008] also report good overall agreement with balloon-borne ozone measurements made at Fort Sumner, USA. In the upper troposphere limited comparison with Southern Hemisphere Additional Ozonesondes (SHADOZ) indicate that EOSMLS has a positive bias (sometimes up to 100%) in the tropics. A more comprehensive validation against a network of 60 ozonesondes [*Jiang et al.*, 2007] showed EOS MLS retrievals to be in good agreement with ozonesondes between 150 and 3 hPa, but to be around 20% higher than ozonesondes at 215 hPa in middle and high latitudes.

[12] SBUV/2 is a nadir-viewing instrument that infers the ozone vertical profile by measuring sunlight scattered from the atmosphere in the middle ultraviolet. The retrievals are provided in 12 layers but are combined at the European Centre for Medium-Range Weather Forecasts (ECMWF) into 6 layers in order to reduce observation correlations. The 6 layers are 0.1–1 hPa, 1–2 hPa, 2–4 hPa, 4–8 hPa, 8–16 hPa and 16 hPa surface. The horizontal resolution is approximately 200 km. Contributions to the total error include calibration errors (due to instrumental drift), which range from 2% at 100 hPa to 5% at 0.5 hPa, and biases due to solar zenith angle. A change in zenith angle from 30° to 60° can lead to systematic errors of −1% to 1%, dependent on the channel. A comparison with SAGE data shows total root

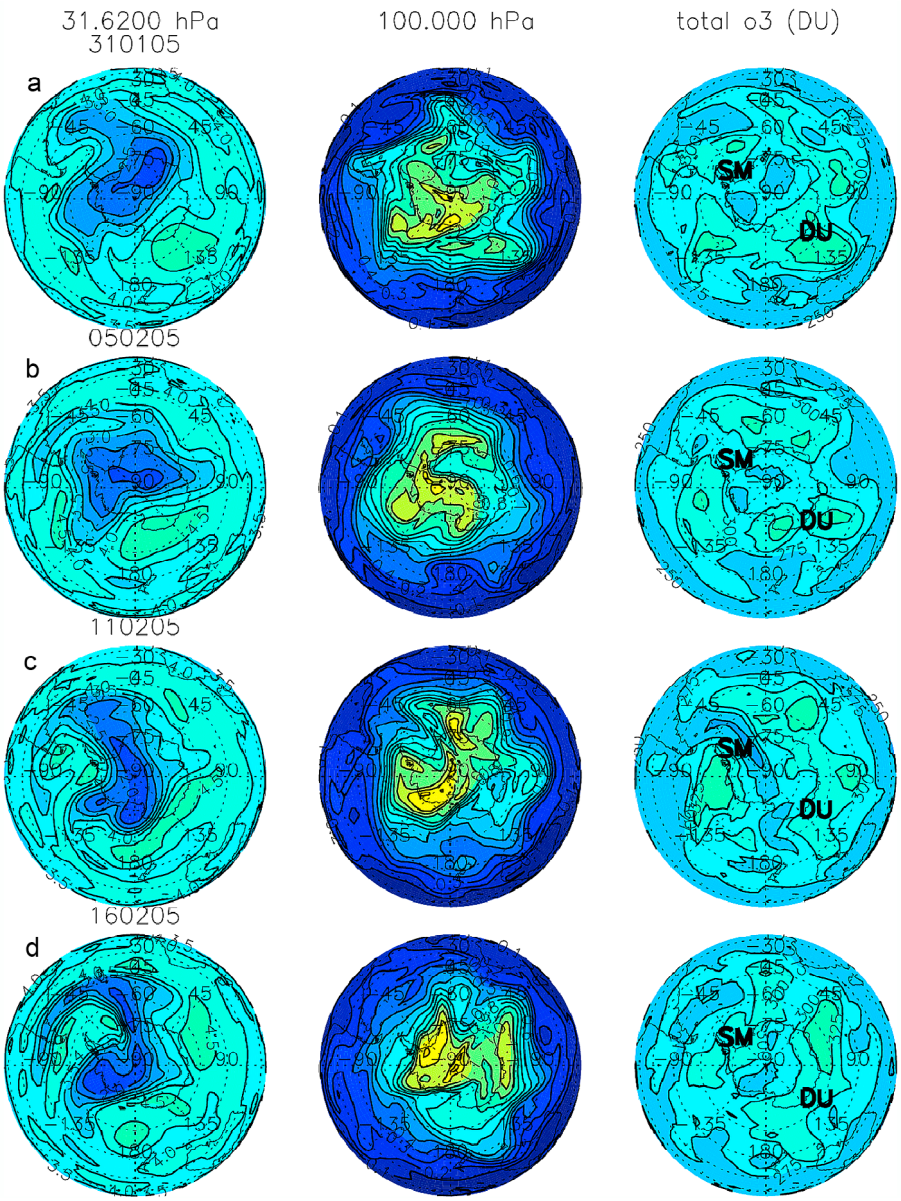

Figure 1. Ozone at (left) 31 hPa, (middle) 100 hPa, and (right) total ozone on (a) 31 January 2005, (b) 5 February 2005, (c) 11 February 2005, (d) 16 February 2005, (e) 25 February 2005, (f) 9 March 2005, and (g) 17 March 2007. "SM" and "DU" on the total ozone plots indicate the locations of San Martin and Dumont d'Urville, respectively. Units are ppmv for pressure level ozone and DU for total ozone.

mean square (rms) errors of 5–15% in the 100–0.3 hPa range [*Bhartia et al.*, 1995, 1996].

[13] In addition, we obtained total ozone data from the Earth Probe Total Ozone Mapping Spectrometer (TOMS) and the Ozone Monitoring Instrument (OMI) on the AURA satellite platform (ftp://toms.gsfc.nasa.gov/pub/omi/data/ozone/) for comparison purposes. All total ozone data were computed from the same OMI-TOMS algorithm vn 8.

2.2. Met Office Assimilation System

[14] The ozone assimilation system is based on a 3D-Var version of the operational Met Office assimilation system [*Lorenc et al.*, 2000], and uses a forecast model which is semi-Lagrangian with a height-based vertical coordinate [*Davies et al.*, 2005]. The model version used here has a horizontal resolution of 3.75° longitude by 2.5° latitude and 50 levels in the vertical, from the surface to around 63 km. EOS MLS and SBUV/2 ozone data are assimilated, together with meteorological observations from satellites, aircraft, radiosondes and surface stations. Further details of the ozone assimilation scheme and the impact of the assimilation of EOS MLS and SBUV/2 data on ozone analyses are noted by *Jackson* [2004, 2007], *Jackson and Saunders* [2002], and *Geer et al.* [2006a, 2006b, 2007].

[15] The assimilation was run for three periods: (1) 26 January 2005 to 10 March 2005, (2) 2 January 2006 to 15 February 2006, and (3) 10 January 2007 to 20 March 2007. These experiments were originally designed for other

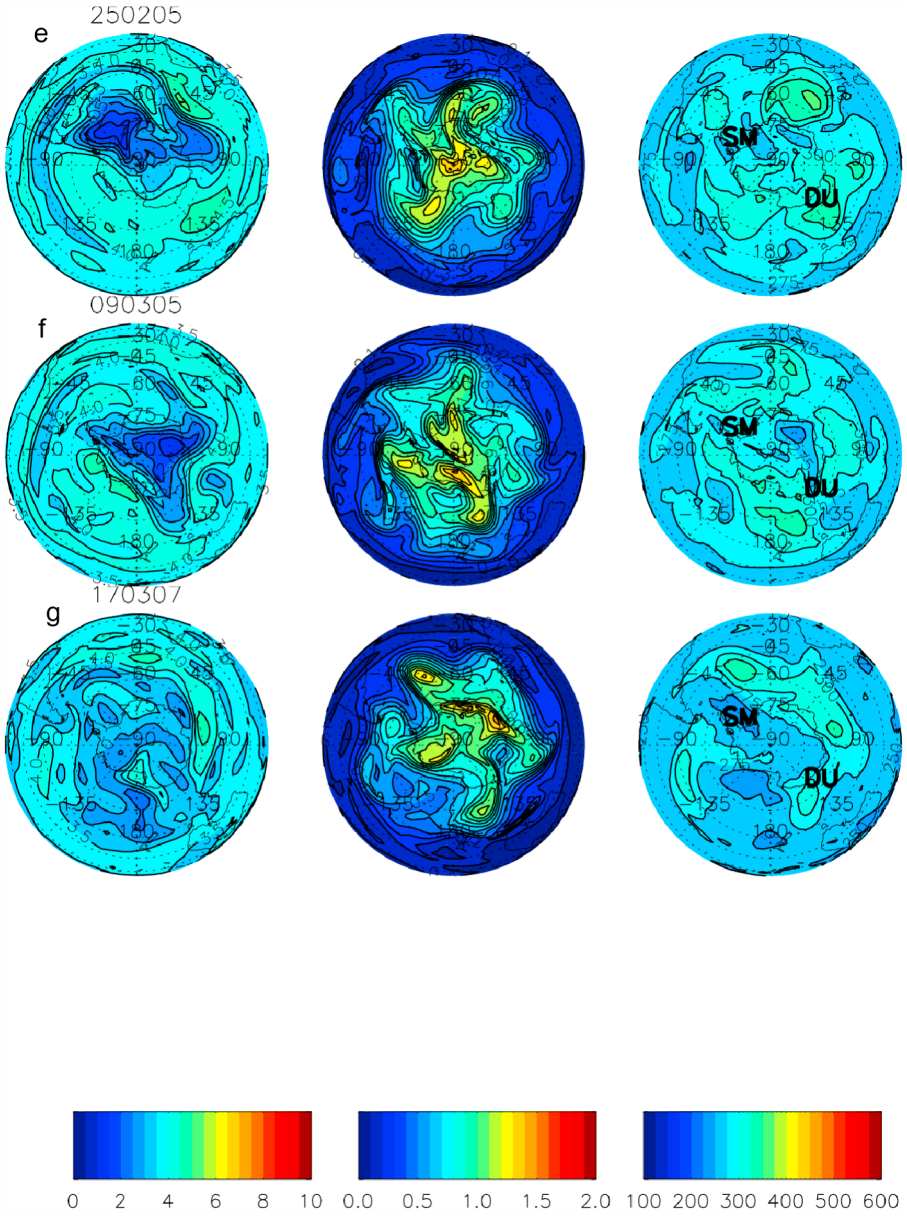

Figure 1. (continued)

purposes, and the investigation of LOEs has followed later. These experiments were run on a supercomputer that is now decommissioned, which means that extending the period of the experiments, or extending them to other years, is difficult.

2.3. UV Data and Dose Calculation Method

[16] We simulated UV indices for clear sky using the FastRT ultraviolet radiation simulation tool [*Engelsen and Kylling*, 2005]. The UV Index is the erythemal dose rate at local solar noon in mW m^{-2} divided by 25. The erythemal dose rate is defined as the integral of the UV spectral irradiances (290–400 nm) incident at a horizontal surface weighted by the standard erythemal action spectrum [*MacKinley and Diffey*, 1987]. When assessing the effect of ozone variations on the UV-B dose, we assumed ideal conditions with no aerosols and a black, nonreflecting surface, and used column ozone amounts from OMI. The OMI total ozone shown here, and the OMI ozone used in the UV Index calculation, excludes observations pertaining to solar zenith angles greater than 85°.

3. Low-Ozone Events in the Southern Polar Stratosphere in Late Summer 2005

3.1. Synoptic Description

[17] We first illustrate that there is significant transport from the polar regions to the lower latitudes in the SH midstratosphere. Figure 1 illustrates the evolution of the LOE during the course of the analysis, using ozone fields at

31 hPa from 6 days during the analysis period. On all days, ozone is lowest over or near the pole. Here, ozone is less than 2.0 ppmv. Tongues of low ozone are also seen, which extend to lower latitudes. On 31 January 2005, two tongues are present. One extends northward from the pole across the Atlantic and westward toward South America. The second tongue, which is less pronounced, extends northward from the pole across the Pacific and westward over New Zealand. These features are related to the presence of anticyclones located over the southern tip of South America and to the south of Australia.

[18] By 5 February 2005, the first tongue has thinned and extended over central Argentina and Chile and the second has deepened slightly over New Zealand. On 11 February 2005 the tongues in these locations are similar to those on 5 February 2005, but the shape of the low-ozone structure over the pole changes, indicating a change in the polar vortex shape and associated transport. After 15 February 2005, the low-ozone tongue in the south Atlantic and central Argentina and Chile is deeper than on previous days. The second tongue over the Pacific is still present on these days but is not generally stronger than on the previous dates. Even near the end of the run (9 March 2005) the tongue of low ozone over South America is clearly seen and is at least as large as tongues of low ozone at other midlatitude locations.

[19] The ozone pattern at 100 hPa is different to that at 31 hPa. Ozone is greatest near the pole, since the chemical ozone loss seen at 31 hPa is not important at 100 hPa and, instead, the ozone distribution is largely controlled by transport. At middle to high latitudes, especially in the latitude belt 45°S–60°S, the ozone field is distorted by the medium-scale quasi-stationary waves (zonal wave number 4–6 or so) [e.g., *Schoeberl and Krueger*; 1983; *Randel and Stanford*, 1985; *Cariolle and Deque*, 1986]. There is also evidence of poleward (equatorward) transport of ozone-poor (rich) air from lower (higher) latitudes, associated with the quasi-stationary ridges and troughs. A prominent poleward intrusion over the Weddell Sea is most evident on 11 February 2005. However, on all 6 days in 2005 shown in Figure 1, there is a broadly similar pattern of poleward transport near the southern tip of South America, south of New Zealand and southeast of South Africa.

[20] Column ozone variability is strongly affected by UTLS dynamics, but nevertheless, ozone variations in the midstratosphere (near 30 hPa) have an impact on column ozone too. That is suggested by Figure 2, which shows time evolution of ozone partial pressure, calculated from our analyses, above a station near the tip of South America, Comodoro Rivadavia, and one across on the Antarctic coast, San Martin. It is apparent that "dents" near 30 hPa, or approximately 25 km, are located well into the main ozone layer, and can hence strongly contribute to the total ozone reduction. Such low-ozone tongues occur repeatedly at 31 and 100 hPa, as evidenced by both Figure 1 and Figure 2, and they occasionally overlay each other. Tongues of low total ozone are often collocated with these low-ozone tongues (Figure 1); this is most obviously seen on 11 February 2005. Another such example is seen to the southwest of South America on 25 February 2005. In addition, on all 6 days in 2005 shown in Figure 1 local total ozone minima to the south of South America, New Zealand and South Africa generally show some deal of correspondence with similar local minima in ozone mixing ratio seen at 100 hPa.

[21] The temporal variation of total ozone from our analyses at selected locations is shown more fully in Figure 3. It already appears clear from Figure 1 that ozone is often lower near the southern tip of South America than at other locations. This is confirmed by Figure 3: a comparison of total ozone at locations around the edge of the Antarctic continent shows that total ozone at San Martin (which is a similar longitude to South America) is frequently less than 300 DU and on two occasions is less than 260 DU, whereas at Dumont D'Urville, which is approximately 180° around the latitude circle from San Martin, total ozone is rarely less than 300 DU. For reference, the locations of Dumont D'Urville and San Martin are also noted on the total ozone maps in Figure 1.

[22] For stations located in populated areas between 40 and 45°S, total ozone over South America (Comodoro Rivadavia) is generally lowest, most clearly near 11 February 2005 and 25 February 2005 (dates which have already been discussed above). Figure 3 shows that total ozone there is below 280 DU for almost the whole of February but, by comparison, total ozone at Hobart drops below 280 DU during this period only infrequently.

3.2. Role of Dynamics in the LOEs

[23] Clearly, stratospheric dynamics play an important role in determining the structure of these low-ozone features. Figure 1 suggests that many of the low total ozone events are likely due to the superposition of equatorward (poleward) transport of low ozone at 31 (100) hPa. Throughout the summer the flow at 100 hPa is generally cyclonic. In the summer at 31 hPa, the flow is characterized by a circumpolar westward circulation, but the anticyclone breaks in January to early February (Figure 4), and by mid-February, two large anticyclones are seen to interact, the one near the tip of South America "feeding" on the remnant of the main anticyclonic summer vortex. This may make the equatorward transport of low ozone at that level more likely, as will the associated rapid rise in the location of the zero wind line from lower to upper stratosphere during that month.

[24] A comparison of ozone and geopotential height fields at 31 and 100 hPa during the first LOE of 11 February 2005 (Figures 1 and 4) is instructive in helping to explain the low total ozone tongues seen on that date. The anticyclone situated near the southern tip of South America at 31 hPa acts to transport low-ozone air from the pole over central/southern Argentina and Chile. At 100 hPa, in that sector, there is a large cyclonic trough, which is highly variable, and the anticyclone is farther north and east than at 31 hPa. The anticyclone and trough are part of the medium-scale (wave number 4–6) pattern of quasi-stationary waves, mentioned before. Since the anticyclone is located farther east at 100 hPa, then over the tip of South America, advection by the anticyclone results in transport of ozone poor air from lower latitudes. Similar advection of ozone poor air from high (low) latitudes at 31 hPa (100 hPa) is also seen over the Pacific. Therefore superposition of equatorward and poleward transport at the two levels (as mentioned above) does appear to be happening and does seem to explain the low tongue of total ozone seen in Figure 3. This

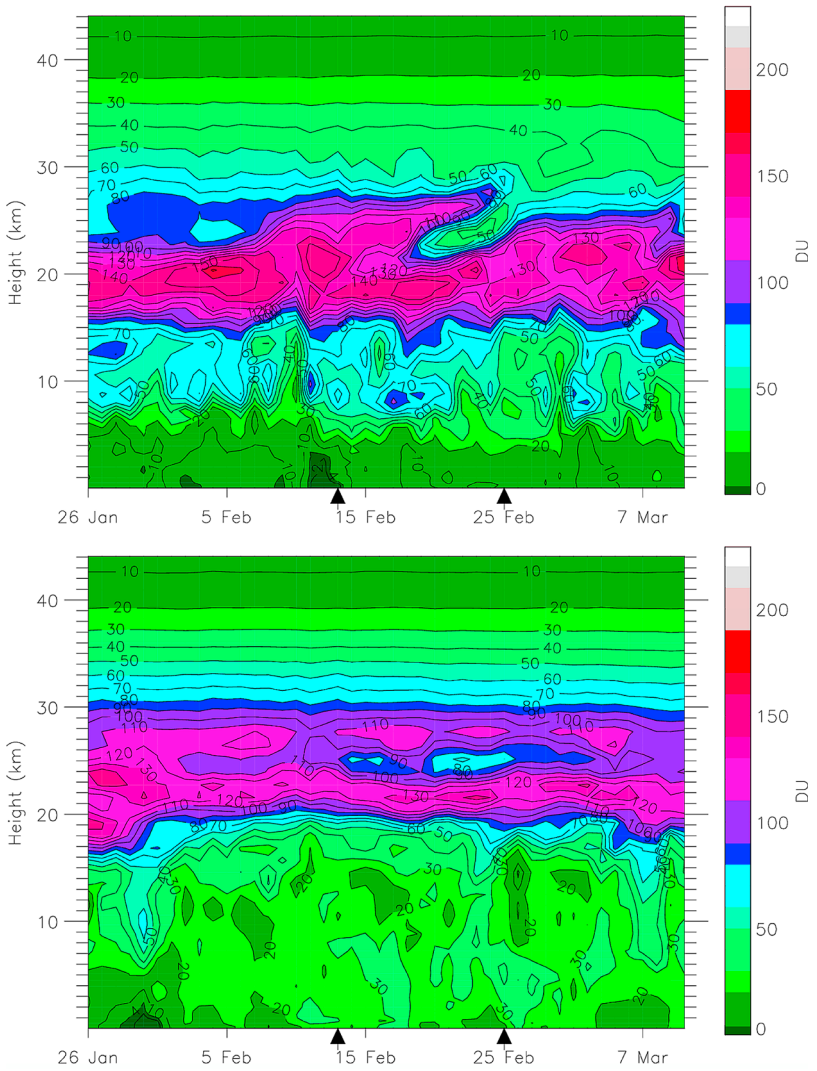

Figure 2. Ozone Partial pressure at (top) San Martin (68.13°S, 67.11°W) and (bottom) Comodoro Rivadavia (45.80°S, 67.50°W) from 26 February 2005 to 10 March 2005. The LOE events on 11 February 2005 and 25 February 2005 discussed in the text are indicated by arrows. Units are ppmv hPa.

may also be happening on 25 February 2005 (not shown), although this is less clear cut and, at 31 hPa in particular, the low-ozone tongue over South America may be residue from previous transport.

[25] This and other examples show that the anticyclones thought important for transport slope poleward and westward with height. This slope enables low-ozone features at 100 and 31 hPa to be superimposed on each other. Examination of other daily plots shows that the anticyclones develop and decay over a period of a few days. This suggests that bursts of baroclinic wave activity are playing an important role. These features are seen throughout much of the experimental period (not just around 11 and 25 February 2005) and at other geographical locations than South America.

[26] Further insight can be obtained by band-passing geopotential height fields to select fluctuations between the synoptic and seasonal scales, following the approach of *Nishii and Nakamura* [2004, 2005] and *Orsolini and Nikulin* [2006]. A low band-pass filter is first applied to daily Met Office analyses to remove periods less than 8 days, and then anomalies are calculated between the filtered field and the 31 day running mean (note that the analyses used are operational Met Office ones, rather than the ones produced by the experiments; however, given that the assimilation system used to produce both sets of analyses is very similar, differences between the two analyses are very small). Figure 5 shows Hovmuller plots of filtered geopotential height anomalies at selected pressure levels and latitudes.

[27] Figure 5 shows the presence of medium-scale (wave number 3 or 4), eastward propagating waves at 316 and 100 hPa at 45°S and 60°S. This is consistent with the waves reported by *Cariolle and Deque* [1986] and *Randel and Stanford* [1985]. There is also some evidence of westward waves in January and early February at 60°S. Similar waves have been identified in Global Positioning System Radio Occultation (GPSRO) data during December 2006 to February 2007 by *Shepherd and Tsuda* [2008]. At 31 hPa at 60°S the pattern of eastward and westward waves is quite similar to that at lower levels. However, the waves at 45°S

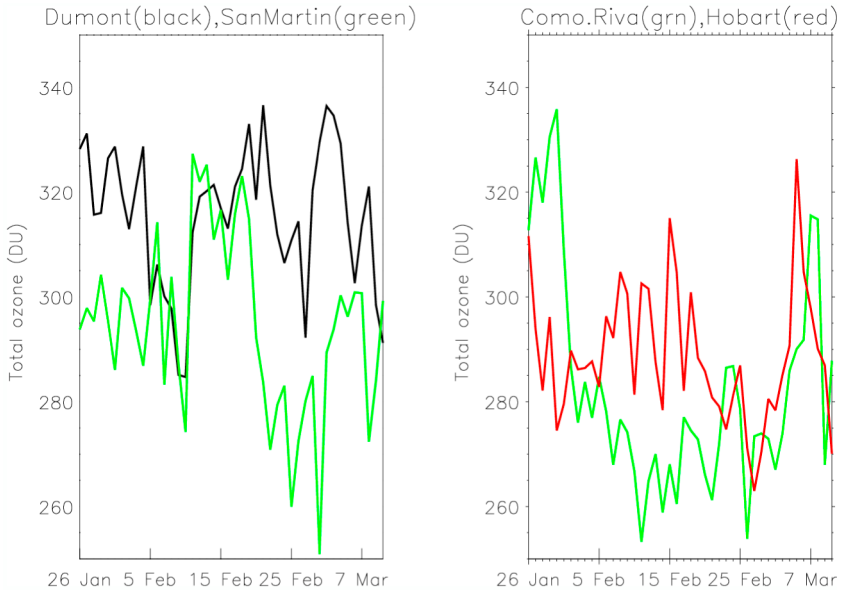

Figure 3. Time series of total ozone for 26 January 2005 to 10 March 2005. (left) Dumont D'Urville (66.07°S, 140.02°E) (black) and San Martin (68.13°S, 67.11°W) (green). (right) Comodoro Rivadavia (45.80°S, 67.50°W) (green) and Hobart (42.82°S, 147.50°E) (red).

are now predominantly westward. At 60°S, anticyclones are initially the remnants of the (anticyclonic) summer vortex and, at 45°S and 60°S, the most intense anticyclones are later present over either South America or the Pacific, which are the locations where low-ozone tongues at 31 hPa are present. The displacement of the upper-level low-ozone pool may thus be related to the occurrence of ultralong stationary or slowly westward-propagating waves.

[28] The Hovmuller plots show a strong correlation in pressure level. Between 316 and 100 hPa the correlation is 0.89 at 60°S and 0.86 at 45°S. Between 100 and 31 hPa it is 0.88 at 60°S but 0.75 at 45°S. This gives credence to the fact that the tropospheric and stratospheric dynamics are connected, while also confirming the increasing importance of westward waves at 45°S between 100 and 31 hPa.

[29] Figure 6 shows a further example of the connection between tropospheric and stratospheric dynamics. In the example shown, an anticyclone develops on 6 February 2005 around 300° and 350 hPa. Over the next 5 days the anticyclone grows in strength around this location, but it also extends quickly upward to the stratosphere by 7 February 2005, and in the subsequent 4 days rapidly strengthens in the stratosphere at all heights below the zero wind line. It is associated with the rapid buildup of the Southern America anticyclone at 30 hPa, feeding from the main vortex remnant (Figure 4). It also tilts westward with height, indicating its baroclinicity. In the next few days this anticyclone rapidly weakens in the stratosphere (not shown), indicating the transient nature of such waves.

[30] Similar plots to Figure 6 show the importance of the location of the zero wind line in controlling the vertical extent of such waves. In January at 60°S the zero wind line is typically located at around 30–40 hPa, compared to 10–20 hPa in February, which explains why low-ozone tongues in that month at 31 hPa are less prominent than in February or March (Figure 1). In addition, at 45°S the zero wind line in February is around 30 hPa and there is little or no wave motion above that level. This can explain why the low-ozone tongues seen in Figure 1 do not tend to extend equatorward of around 45°S and instead get increasingly elongated with time at that latitude. This indicates transport by the zonally symmetric, rather than eddy, flow.

4. LOEs in 2006 and 2007

[31] Figure 7 is similar to Figure 3, except total ozone values from 2006 and 2007 are shown. A striking result is that in both these years, as with 2005, total ozone at San Martin is clearly lower than at Dumont d'Urville. Total ozone at San Martin is frequently less than 300 DU, and at Dumont d'Urville it is usually greater than 300 DU, at least up until early March. A difference from 2005 is that there appears to be more of a decrease in total ozone with time in 2006 and 2007.

[32] To investigate whether this feature is present in other years, in Figure 7 we also show the February–March mean total ozone from the combined TOMS and OMI record for 1997–2007 (a combination required because the EarthProbe TOMS instrument ceased operations in 2005 and OMI was only launched in 2004). The TOMS/OMI fields reveal a pronounced crescent-like zonal asymmetry around 60°S, with lower total ozone in the western hemisphere than the eastern. Furthermore, between around 65°S and 70°S, there is a minimum in total ozone located near the Antarctic Peninsula. This is a region where the radius and density of surface cyclones are lower in summer [*Yuan et al.*, 2009]. Similar patterns are seen in 1979–1992 Nimbus 7 TOMS total ozone data (not shown), indicating the climatological robustness of the results. The pattern in the TOMS/OMI total ozone record is consistent with what is shown in the total ozone time series for 2005–2007 at San Martin and Dumont d'Urville. Another crescent-like zonal asymmetry

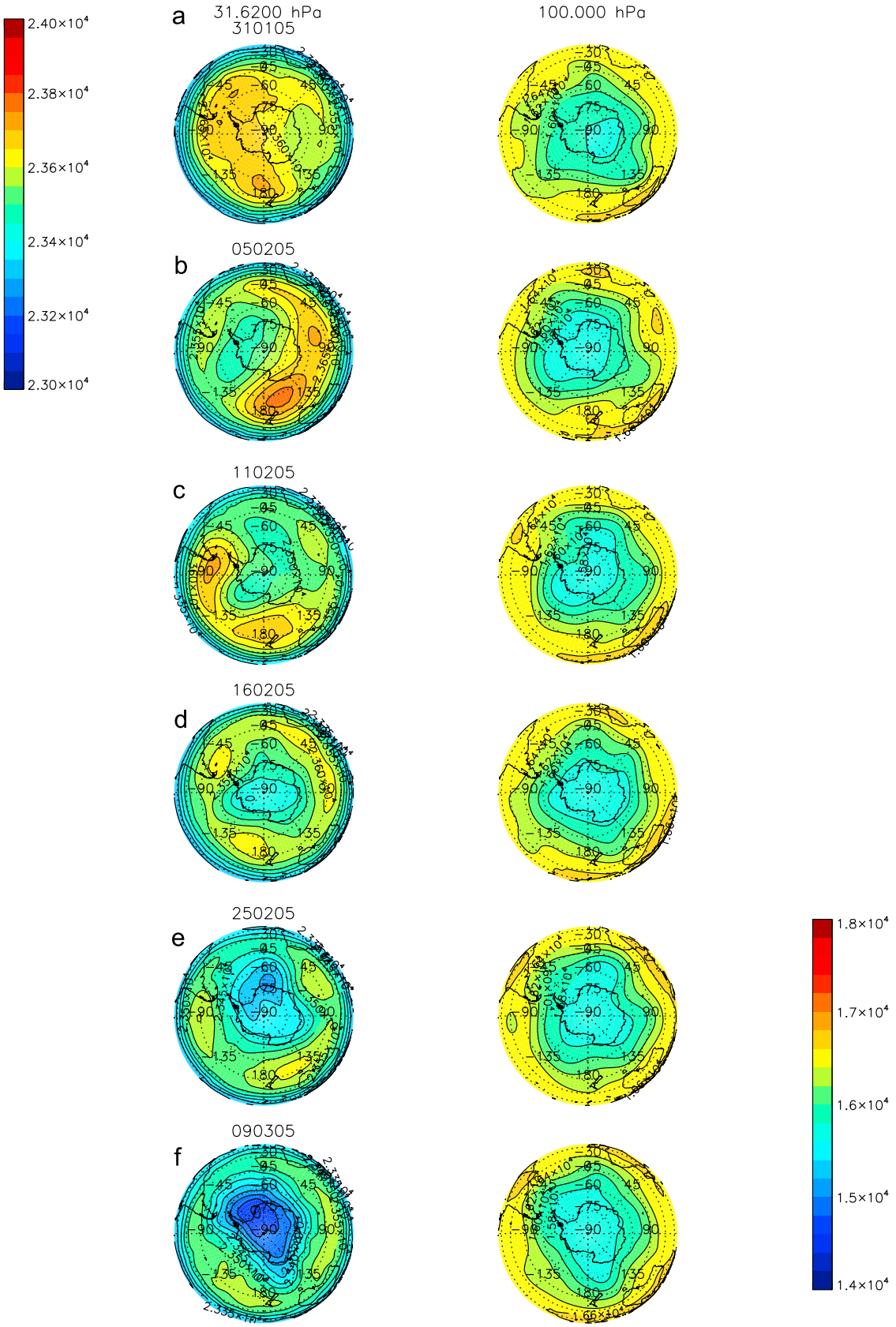

Figure 4. Geopotential height at (left) 31 hPa and (right) 100 h Pa for (a) 31 January 2005, (b) 5 February 2005, (c) 11 February 2005, (d) 16 February 2005, (e) 25 February 2005, (f) 9 March 2005. Color bars for the 31 hPa and 100 hPa plots are shown on the top left and bottom right, respectively. Units are meters.

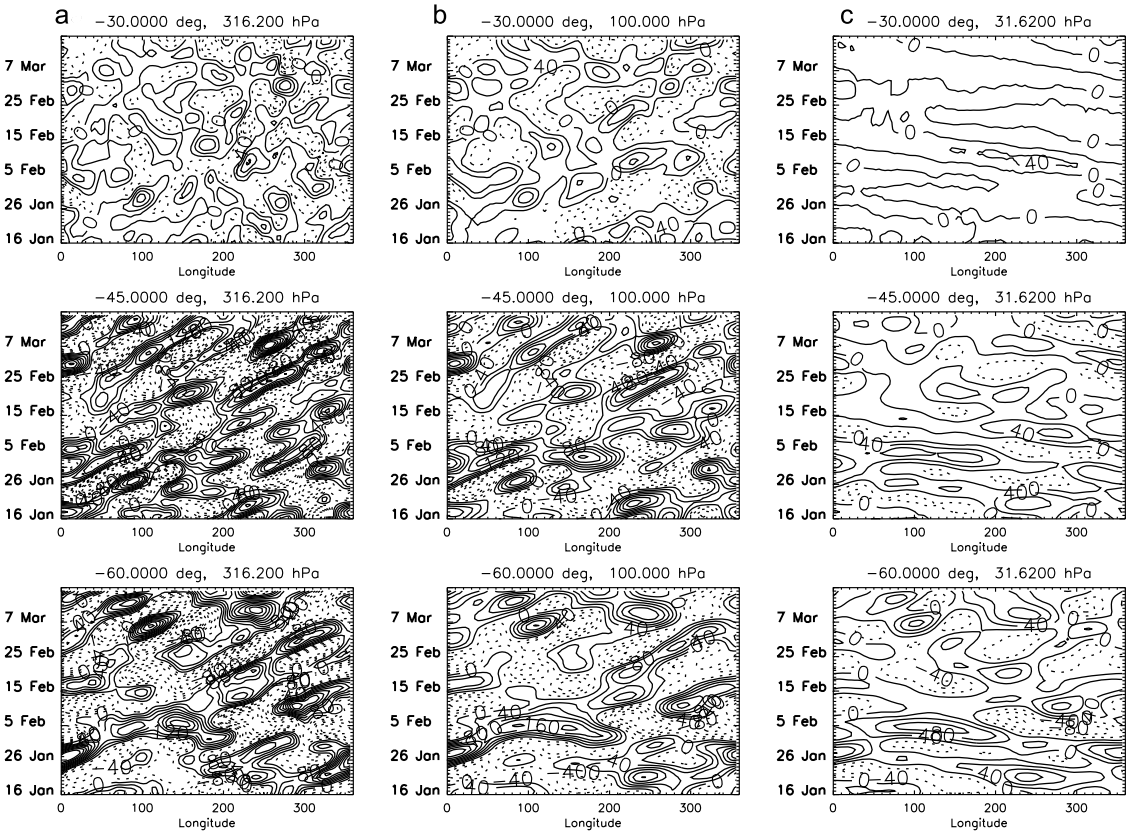

Figure 5. Hovmuller plot of filtered geopotential height anomaly from 16 January 2005 to 16 March 2005 at (a) 316 hPa, (b) 100 hPa, and (c) 31 hPa and (top) 30°S, (middle) 45°S, and (bottom) 60°S. Units are meters.

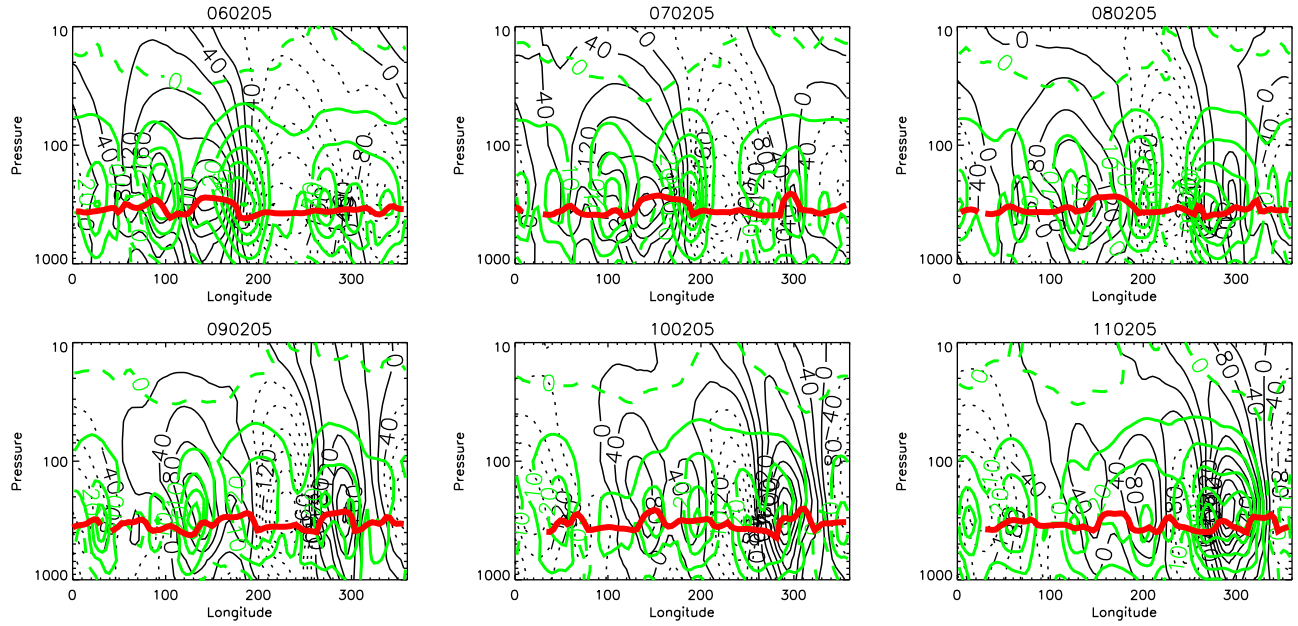

Figure 6. Longitude/pressure section at 60°S from 6 February 2005 to 11 February 2005 of filtered geopotential height (black), zonal wind (green), and 2 PVU tropopause (red). Zero-wind line is indicated by green dashed line.

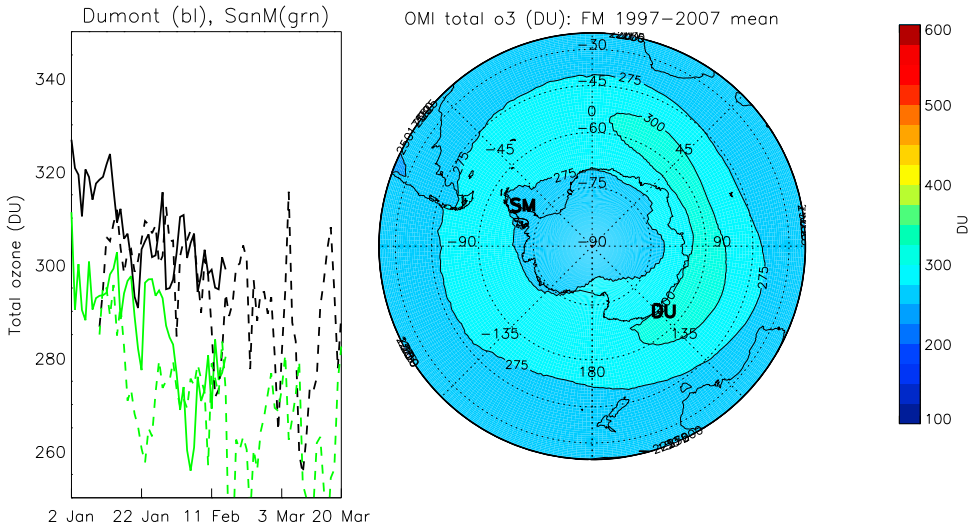

Figure 7. (left) Total ozone for 2006 (solid line) and 2007 (dashed line) for 2 February to 20 March period for Dumont D'Urville (66.07°S, 140.02°E) (black) and San Martin (68.13°S, 67.11°W) (green). (right) Mean February–March TOMS/OMI total ozone for 1997–2007. Units are DU.

has been noted [e.g., *Hitchman and Rogal*, 2010, and references therein], but in that case it occurs between August and October and the ozone maximum is located south of Australia.

[33] Our results show that there are considerable similarities between the ozone fields in 2005 and 2006. This can be at least partially explained by the fact that throughout January and February in both years the zero wind line at middle to high latitudes is located at a similar level (30–40 hPa). This suggests that the potential for wave propagation to the lower stratosphere is similar in both years. Accordingly, we do not discuss the results for 2006 in any more detail.

[34] Hovmuller plots of filtered geopotential height for 2007 (not shown) are fairly similar to those for 2005 (Figure 5) and 2006 (not shown). However, an examination of LOEs via pressure level plots reveals that the LOEs in 2007 do differ from the other 2 years studied, although the difference is still quite slight. For example, during January the ozone minimum over the pole at 31 hPa is less distinct and the meridional gradient at high latitudes is accordingly often less strong. Furthermore, in February and March 2007, although ozone at 31 hPa is still low near the Weddell Sea, as in 2005 and 2006, there is also a prominent polar ozone minimum over the Ross Sea, and the Pacific low-ozone tongue tends to be located south of Australia rather than to the east of New Zealand. An example of this is shown in Figure 1 for 17 March 2007. This difference is related to the fact that the major anticyclones seen at 31 hPa in February 2007 are typically located farther west than those in 2005 (Figure 4) or 2006. These anticyclones are remnants of the summer anticyclonic vortex, and their locations may depend on the details of the processes responsible for the breakup of that vortex.

[35] *Shepherd and Tsuda* [2008] suggested that the planetary wave activity they reported, and which we also see here, may be related to the breaking of the Antarctic winter polar vortex around November or December. It is noted that the vortex breaks down around the same time in 2004/2005 and 2005/2006, but slightly later in 2006/2007. One may speculate that this could be a reason why the LOEs in February 2005 and 2006 are similar, but those in February 2007 differ slightly. In any event, although our results show that there is interannual variability in the characteristics of the LOEs, clearly 3 years is not enough to draw any firm conclusions on such variability.

5. Impact on UV Radiation

[36] The LOEs have a strong effect on the surface UV radiation, compared to the mean surface UV for that latitude, as was the case for northern hemisphere summer LOEs [*Orsolini et al.*, 2003]. Figure 8 shows OMI total ozone and UV Index anomaly (for that latitude and time of year), on 11 February 2005, 25 February 2005 and 17 March 2007. It dramatically shows the localized region of enhanced UV Index dose in the low-ozone tongue stretching toward the South Pole and especially over the Weddell Sea. Locations there get around 20–30% more UVB than the zonal mean, and locations near the tip of South America 10–25% more.

[37] The longitudinal distribution of the UV Index for February 2005–2007 is shown in Figure 9. The longitudinal structure mirrors the crescent-like ozone structure to first order. In addition the highest UV Index (greater than 4.0) at 64.5°S is chiefly in the 20°W–100°W region, This region includes the Antarctic Peninsula/Weddell Sea and Pacific areas where LOEs are reported above.

[38] The UV Index is the most widely reported quantity for ultraviolet radiation. It represents the efficiency of sunburn of human skin at solar noon. For a UV Index of 3–5 the general recommendation is "Wear sunglasses and use SPF 15+ sunscreen, cover the body with clothing and a hat, and seek shade around midday when the Sun is most intense." [(EPA SunWise: UV Index, http://epa.gov/sunwise/uvindex.html).

[39] Phytoplankton photosynthetic rates decrease sharply in surface waters where cells are exposed to UV radiation due to inhibition. A UVB threshold of 0.5–0.75 W m^{-2} exist

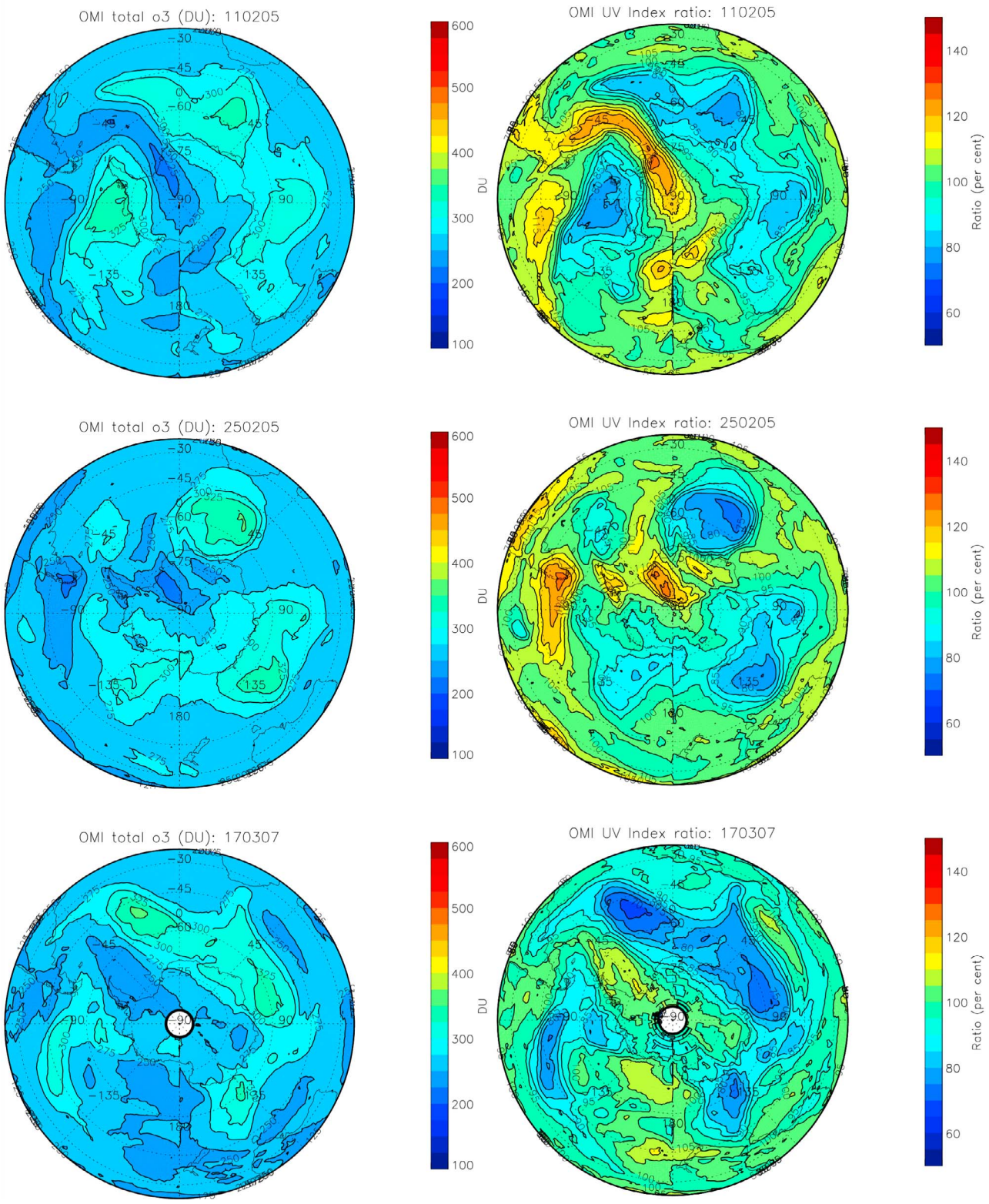

Figure 8. Total ozone from (left) OMI. (right) Ratio of UV Index simulated from the local and zonal mean (<−20°S) total ozone. (top) Fields for 11 February 2005. (middle) Fields for 25 February 2005. (bottom) Fields for 17 March 2007. Units are DU for total ozone and percent for UV Index. Note that there is a discontinuity in the fields near the dateline. This is because the OMI data are retrieved from different satellite overpasses under changing atmospheric conditions and do not represent a snapshot picture.

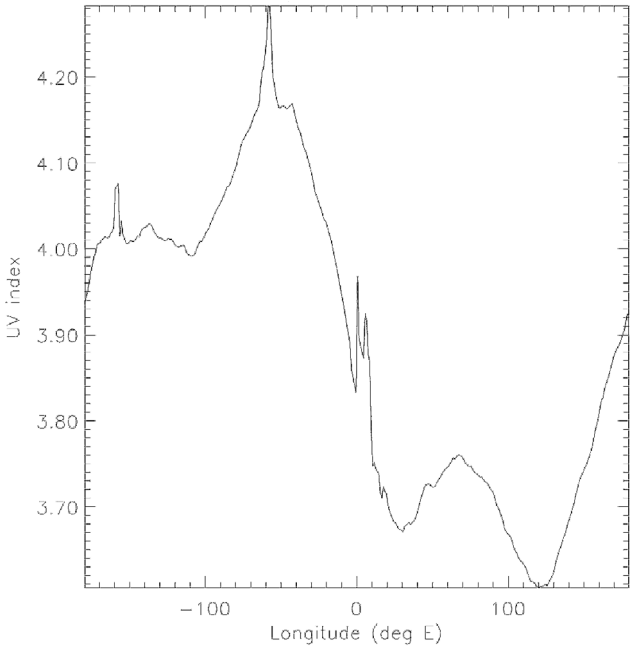

Figure 9. Mean February UV Index for 2005–2007 at 64.5°S calculated from OMI data.

for photosynthetic inhibition to phytoplankton in Antarctic coastal waters [*Smith and Cullen*, 1995; *Helbling and Villafane*, 2002; *Zhou et al.*, 2009]. In mid-February under clear-sky conditions at 64.5°S and an ozone column of 410 (310) DU a threshold of 0.50 (0.75) W m^{-2} would correspond to a UV Index of 2.5 (3.5). Reducing the ozone column from 325 DU to 225 DU (Figure 8) extends the daily duration of photosynthetic inhibition at the ocean surface (i.e., when UVB > 0.5 W m^{-2}) from 5.5 h to 7.7 h. Figure 9 shows that the UV indices in the Antarctic summer exceed the lower levels for UV protection for humans and photosynthetic inhibition of phytoplankton.

6. Summary and Discussion

[40] In this paper, we examined LOEs in the southern summer stratosphere from ozone analyses produced using the Met Office ozone data assimilation system. Ozone data from EOS MLS and SBUV/2 were assimilated and experiments were performed for January–March 2005, 2006 and 2007 using the Met Office ozone data assimilation system.

[41] Our results show that at 31 hPa in February tongues of low-ozone air are pulled out of the polar region and extend to lower latitudes. These tongues are most prominent over the southern tip of South America and the Pacific and the patterns have many similarities in all 3 years studied. Low tongues at these locations are also seen at 100 hPa, but in this case transport of low ozone from low to high latitudes is taking place. Low tongues at both levels are frequently superimposed on one another, meaning that there are often also reductions in total ozone. What is striking from our results and from OMI total ozone analyses is that around the edge of the Antarctic, total ozone throughout January to March is typically lower over the Weddell Sea than at other longitudes.

[42] The low-ozone tongues at 31 (100) hPa are consistent with equatorward (poleward) transport of low ozone to lower (higher) latitudes by planetary wave activity. Daily geopotential height fields show that anticyclonic circulations that contribute to these patterns tilt poleward and westward with height, and develop and decay over the period of a few days. This indicates the important role that baroclinic waves play and also the slope with height enables low-ozone features at 100 and 31 hPa to be superimposed on each other.

[43] Examination of filtered geopotential height anomalies reveals the presence of waves reported in other studies and indicates the clear connection between tropospheric and stratospheric wave dynamics in driving such summertime LOEs. There are medium-scale (wave number 3 or 4), eastward propagating waves present at 316 and 100 hPa at 45 and 60°S. This is consistent with the waves reported by *Cariolle and Deque* [1986] and *Randel and Stanford* [1985]. At 31 hPa at 60°S the pattern of waves is quite similar to that at lower levels, but at 45°S there is a switch to a predominantly westward pattern. The displacement of the upper-level low-ozone pool may thus be related to the occurrence of ultralong stationary or slowly westward-propagating waves. Such waves have been observed in summer 2006/07, in GPSRO temperature observations at high southern latitudes [*Shepherd and Tsuda*, 2008].

[44] An important question is whether the Weddell Sea is a preferred region for such LOEs. Clearly, 3 years is insufficient to comment on the robustness of this feature, and therefore a follow-on study which was based on a much longer duration data set, such as ECMWF reanalyses, would be desirable. There is little indication from the literature as to why total ozone tends to be lower in the Weddell Sea area, or why LOEs seem to form frequently in this region. One clue comes from *Yuan et al.* [2009], who used ECMWF analyses from 1999 to 2006 to show that the radius and density of surface level cyclones is lower in southern summer over the Weddell Sea than at other locations around the same latitude circle. This may indicate by corollary a higher frequency of surface anticyclones over the Weddell Sea which might also lead to a higher frequency of anticyclones near 100 hPa, which would then contribute to, as discussed in this paper, low ozone in the stratosphere. Further support comes from *Cariolle and Deque* [1986], who show variations in the squared amplitudes of wave number 4–6 waves which appear well correlated in time between the 700, 300 and 100 hPa. However, phase differences between these levels were not discussed, and our argument for a linkage between the surface and lower stratosphere anticyclones over the Weddell Sea assumes an equivalent barotropic structure throughout the troposphere, and then a transition to a baroclinic structure (consistent with the results presented in this paper) in the stratosphere. It is not clear how frequently the barotropic structure exists, and further investigation is required to find the answer to this question.

[45] There is also a high correlation between the regions of low total ozone and UV radiation. Figure 8 shows an increase in UV Index over the Weddell Sea, and, in addition, parts of the Antarctic coastline near the Weddell Sea have a UV Index that is around 20–30% greater than the zonal mean, and the tip of South America about 10–25% greater. The Antarctic Peninsula and Weddell Sea make up the most

diverse and productive Antarctic marine ecosystem, and thus it is important to understand the impact of increases in UV on this ecosystem. UV radiation is known to affect strongly phytoplankton [e.g., *Smith et al.*, 1992] and some studies have documented increased UV radiation in the Weddell Sea in spring [e.g., *Lubin et al.*, 2004] and the associated photoinhibition in Antarctic plankton. *Smith et al.* [1992] found that the Antarctic springtime ozone depletion of the ozone column from 300 DU to 200 DU could reduce the primary production in the marginal ice zone by at least 6–12%. Later studies indicate positive impacts of ozone depletion on aquatic primary production [*Hamre et al.*, 2008]. Most such studies have, understandably enough, focused on Antarctic spring, where ozone depletion is larger. Now that this study has served to document the existence of summertime LOEs, it may be worthwhile to extend studies of the impact of enhanced UV radiation on the marine ecosystem to summer, especially since, in the Antarctic, the UV Index during the summertime LOE events is similar to the UV Index during the springtime ozone hole. It is unclear what kind of impact these short-term UV variations in a season of strong UV fluxes, albeit large, would have on ecosystems, though it is worth pointing out that the impact may be magnified by the lower sea ice amounts present in the Weddell Sea in summer. The impact of UV fluxes on primary production is not necessarily the same as during spring [*Smith et al.*, 1992] because the vertical profiles of phytoplankton are much more variable after the initial spring bloom in the marginal ice zone [e.g., *Engelsen et al.*, 2002].

[46] **Acknowledgments.** We thank the ozone processing team at NASA GSFC code 613.3 for providing free access to TOMS and OMI data. Y.O.R. and O.E.N. were partly supported by the Norwegian Space Centre (project SATLUFT).

References

Allen, D. R., and N. Nakamura (2002), Dynamical reconstruction of the record low column ozone over Europe on 30 November 1999, *Geophys. Res. Lett.*, *29*(9), 1362, doi:10.1029/2002GL014935.

Bhartia, P. K., S. Taylor, R. D. McPeters, and C. Wellemeyer (1995), Application of the Langley plot method to the calibration of the solar backscattered ultraviolet instrument on the Nimbus 7 satellite, *J. Geophys. Res.*, *100*, 2997–3004, doi:10.1029/94JD03072.

Bhartia, P. K., R. D. McPeters, C. L. Mateer, L. E. Flynn, and C. Wellemeyer (1996), Algorithm for the estimation of vertical ozone profiles from the backscattered ultraviolet technique, *J. Geophys. Res.*, *101*, 18,793–18,806, doi:10.1029/96JD01165.

Canziani, P., R. H. Compagnucci, S. A. Bischoff, and W. E. Legnani (2002), A study of the impacts of tropospheric synoptic processes on the genesis and evolution of extreme total ozone anomalies over southern South America, *J. Geophys. Res.*, *107*(D24), 4741, doi:10.1029/2001JD000965.

Cariolle, D., and M. Deque (1986), Southern Hemisphere medium-scale waves and total ozone disturbances in a spectral general circulation model, *J. Geophys. Res.*, *91*, 10,825–10,846, doi:10.1029/JD091iD10p10825.

Cede, A., E. Luccini, L. Nuñez, R. D. Piacentini, and M. Blumthaler (2002), Monitoring of erythemal irradiance in the Argentine Ultraviolet Network, *J. Geophys. Res.*, *107*(D13), 4165, doi:10.1029/2001JD001206.

Compagnucci, R. H., M. A. Salles, and P. O. Canziani (2001), The spatial and temporal behaviour of the lower stratospheric temperature over the Southern Hemisphere: The MSU view. Part I: Methodology and temporal behaviour, *Int. J. Climatol.*, *21*, 419–437, doi:10.1002/joc.606.

Davies, T., M. J. P. Cullen, A. J. Malcolm, M. H. Mawson, A. Staniforth, A. A. White, and N. Wood (2005), A new dynamical core for the Met Office's global and regional modelling of the atmosphere, *Q. J. R. Meteorol. Soc.*, *131*, 1759–1782, doi:10.1256/qj.04.101.

de Laat, A. T. J., R. J. van der A, M. A. F. Allaart, M. van Weele, G. C. Benitez, C. Casiccia, N. M. Paes Leme, E. Quel, J. Salvador, and E. Wolfram (2010), Extreme sunbathing: Three weeks of small total O_3 columns and high UV radiation over the southern tip of South America during the 2009 Antarctic O_3 hole season, *Geophys. Res. Lett.*, *37*, L14805, doi:10.1029/2010GL043699.

Engelsen, O., and A. Kylling (2005), Fast simulation tool for ultraviolet radiation at the Earth's surface, *Opt. Eng.*, *44*(4), 041012.17, doi:10.1117/1.1885472.

Engelsen, O., E. N. Hegseth, H. Hop, E. Hansen, and S. Falk-Petersen (2002), Spatial variability of chlorophyll-*a* in the Marginal Ice Zone of the Barents Sea, with relations to sea ice and oceanographic conditions, *J. Mar. Syst.*, *35*(1–2), 79–97, doi:10.1016/S0924-7963(02)00077-5.

Froidevaux, L., et al. (2008), Validation of Aura Microwave Limb Sounder stratospheric ozone measurements, *J. Geophys. Res.*, *113*, D15S20, doi:10.1029/2007JD008771.

Geer, A. J., et al. (2006a), The ASSET intercomparison of ozone analyses: Method and first results, *Atmos. Chem. Phys.*, *6*, 5445–5474, doi:10.5194/acp-6-5445-2006.

Geer, A. J., C. Peubey, R. Bannister, R. Brugge, D. R. Jackson, W. A. Lahoz, and A. O'Neill (2006b), Assimilation of stratospheric ozone from MIPAS into a global general circulation model: The September 2002 vortex split, *Q. J. R. Meteorol. Soc.*, *132*, 231–257, doi:10.1256/qj.04.181.

Geer, A. J., W. A. Lahoz, D. R. Jackson, D. Cariolle, and J. P. McCormack (2007), Evaluation of linear ozone photochemistry parametrizations in a stratosphere-troposphere data assimilation system, *Atmos. Chem. Phys.*, *7*, 939–959, doi:10.5194/acp-7-939-2007.

Hamre, B., J. J. Stamnes, O. Frette, S. R. Erga, and K. Stamnes (2008), Could stratospheric ozone depletion lead to enhanced aquatic primary production in the polar regions?, *Limnol. Oceanogr.*, *53*, 332–338, doi:10.4319/lo.2008.53.1.0332.

Helbling, E. W., and V. E. Villafane (2002), UV radiation effects on phytoplankton primary production: A comparison between Arctic and Antarctic marine ecosystems, in *UV Radiation and Arctic Ecosystems*, *Ecol. Stud.*, vol. 153, edited by D. O. Hessen, pp. 203–226, Springer, New York.

Hitchman, M. H., and M. J. Rogal (2010), Influence of tropical convection on the Southern Hemisphere ozone maximum during the winter to spring transition, *J. Geophys. Res.*, *115*, D14118, doi:10.1029/2009JD012883.

Hood, L. L., B. E. Soukharev, M. Fromm, and J. P. McCormack (2001), Origin of extreme ozone minima at middle to high northern latitudes, *J. Geophys. Res.*, *106*, 20,925–20,940, doi:10.1029/2001JD900093.

Huth, R., and P. O. Canziani (2003), Classification of hemispheric monthly mean stratospheric potential vorticity fields, *Ann. Geophys.*, *21*, 805–817, doi:10.5194/angeo-21-805-2003.

Jackson, D. R. (2004) Improvements in ozone data assimilation at the Met Office, *Met Office Forecasting Res. Tech. Rep. 454*, Met Off., Exeter, U. K.

Jackson, D. R. (2007), Assimilation of EOS MLS ozone observations in the Met Office data assimilation system, *Q. J. R. Meteorol. Soc.*, *133*, 1771–1788, doi:10.1002/qj.140.

Jackson, D. R., and R. Saunders (2002) Ozone data assimilation: Preliminary system, *Met Office Forecasting Res. Tech. Rep. 394*, Met Off., Exeter, U. K.

James, P. M. (1998), A climatology of ozone mini-holes over the Northern Hemisphere, *Int. J. Climatol.*, *18*, 1287–1303, doi:10.1002/(SICI)1097-0088(1998100)18:12<1287::AID-JOC315>3.0.CO;2-4.

Jiang, Y. B., et al. (2007), Validation of Aura Microwave Limb Sounder Ozone by ozonesonde and lidar measurements, *J. Geophys. Res.*, *112*, D24S34, doi:10.1029/2007JD008776.

Keil, M., D. R. Jackson, and M. Hort (2007), The January 2006 low ozone event over the UK, *Atmos. Chem. Phys.*, *7*, 961–972, doi:10.5194/acp-7-961-2007.

Kirchhoff, V. W. J. H., Y. Sahai, S. C. A. R. Casiccia, B. S. F. Zamorano, and V. V. Valderrama (1997), Observations of the 1995 ozone hole over Punta Arenas, Chile, *J. Geophys. Res.*, *102*, 16,109–16,120, doi:10.1029/97JD00276.

Lorenc, A. C., et al. (2000), The Met Office global three dimensional data assimilation scheme, *Q. J. R. Meteorol. Soc.*, *126*, 2991–3012, doi:10.1002/qj.49712657002.

Lubin, D., K. R. Arrigo, and G. L. van Dijken (2004), Increased exposure of Southern Ocean phytoplankton to ultraviolet radiation, *Geophys. Res. Lett.*, *31*, L09304, doi:10.1029/2004GL019633.

MacKinley, A. F., and B. L. Diffey (1987), A reference action spectrum for ultraviolet induced erythema in human skin, *CIE J.*, *6*, 17–22.

McKenna, D. S., R. L. Jones, J. Austin, E. V. Browell, M. P. McCormick, A. J. Krueger, and A. F. Tuck (1989), Diagnostic studies of the Antarctic

vortex during the 1987 Airborne Antarctic Ozone Experiment—Ozone miniholes, *J. Geophys. Res.*, *94*, 11,641–11,668, doi:10.1029/JD094iD09p11641.

Newman, P. A., L. A. Lait, and M. R. Schoeberl (1988), The morphology and meteorology of southern-hemisphere spring total ozone mini-holes, *Geophys. Res. Lett.*, *15*, 923–926, doi:10.1029/GL015i008p00923.

Nishii, K., and H. Nakamura (2004), Lower-stratospheric Rossby wave trains in the southern hemisphere: A case study for late winter 1997, *Q. J. R. Meteorol. Soc.*, *130*, 325–345, doi:10.1256/qj.02.156.

Nishii, K., and H. Nakamura (2005), Upward and downward injection of Rossby wave activity across the tropopause: A new aspect of the troposphere-stratosphere dynamical linkage, *Q. J. R. Meteorol. Soc.*, *131*, 544–563, doi:10.1256/qj.03.91.

Orsolini, Y. J., and G. Nikulin (2006), A low-ozone episode during the European heat wave of August 2003, *Q. J. R. Meteorol. Soc.*, *132*, 667–680, doi:10.1256/qj.05.30.

Orsolini, Y., D. B. Stephenson, and F. J. Doblas-Reyes (1998), Storm track signature in total ozone during Northern Hemisphere winter, *Geophys. Res. Lett.*, *25*, 2413–2416, doi:10.1029/98GL01852.

Orsolini, Y. J., H. Eskes, G. Hansen, U.-P. Hoppe, A. Kylling, E. Kyro, J. Notholt, R. Van der A, and P. Von der Gathen (2003), Summertime low ozone episodes over northern high latitudes, *Q. J. R. Meteorol. Soc.*, *129*, 3265–3275, doi:10.1256/qj.02.211.

Pazmiño, A. F., S. Godin-Beekmann, M. Ginzburg, S. Bekki, A. Hauchecorne, R. Piacentini, and E. Quel (2005), Impact of Antarctic polar vortex occurrences on total ozone and UVB radiation at southern Argentinean and Antarctic stations during 1997–2003 period, *J. Geophys. Res.*, *110*, D03103, doi:10.1029/2004JD005304.

Pazmiño, A. F., S. Godin-Beekmann, E. A. Luccini, R. D. Piacentini, E. J. Quel, and A. Hauchecorne (2008), Increased UV radiation due to polar ozone chemical depletion and vortex occurrences at southern sub-polar latitudes in the period [1997–2005], *Atmos. Chem. Phys.*, *8*, 5339–5352, doi:10.5194/acp-8-5339-2008.

Pérez, A., E. Crino, I. Aguirre de Cárcer, and F. Jacque (2000), Low ozone events and three-dimensional transport at midlatitudes of South America during springs of 1996 and 1997, *J. Geophys. Res.*, *105*, 4553–4561, doi:10.1029/1999JD901040.

Peters, D., J. Egger, and G. Entzian (1995), Dynamical aspects of ozone mini-hole formation, *Meteorol. Atmos. Phys.*, *55*, 205–214, doi:10.1007/BF01029827.

Petzoldt, K. (1999), The role of dynamics in total ozone deviations from their long-term mean over the Northern Hemisphere, *Ann. Geophys.*, *17*, 231–241, doi:10.1007/s00585-999-0231-1.

Petzoldt, K., B. Naujokat, and K. Neugeboren (1994), Correlation between stratospheric temperature, total ozone, and tropospheric weather systems, *Geophys. Res. Lett.*, *21*, 1203–1206, doi:10.1029/93GL03020.

Randel, W. J., and J. L. Stanford (1985), An observational study of medium-scale wave dynamics in the Southern Hemisphere summer. Part I: Wave structure and energetics, *J. Atmos. Sci.*, *42*, 1172–1188, doi:10.1175/1520-0469(1985)042<1172:AOSOMS>2.0.CO;2.

Schoeberl, M. R., and A. J. Krueger (1983), Medium-scale disturbances in total ozone during Southern Hemisphere summer, *Bull Am. Meteorol. Soc.*, *64*, 1358–1365.

Shepherd, M. G., and T. Tsuda (2008), Large-scale planetary disturbances in stratospheric temperature at high latitudes in the southern summer hemisphere, *Atmos. Chem. Phys.*, *8*, 7557–7570, doi:10.5194/acp-8-7557-2008.

Smith, R. C., and J. J. Cullen (1995), Effects of UV radiation on phytoplankton, *Rev. Geophys.*, *33*, 1211–1224, doi:10.1029/95RG00801.

Smith, R. C., et al. (1992), Ozone depletion: Ultraviolet radiation and phytoplankton biology in Antarctic waters, *Science*, *255*, 952–959, doi:10.1126/science.1546292.

Yuan, X., J. Patoux, and C. Li (2009), Satellite-based midlatitude cyclone statistics over the Southern Ocean: 2. Tracks and surface fluxes, *J. Geophys. Res.*, *114*, D04106, doi:10.1029/2008JD010874.

Zhou, W., K. Yin, I. Yuan, and X. Ning (2009), Comparison of the effects of short-term UVB radiation exposure on phytoplankton photosynthesis in the temperate Changjiang and subtropical Zhujiang estuaries of China, *J. Oceanogr.*, *65*, 627–638, doi:10.1007/s10872-009-0053-5.

O. Engelsen and Y. J. Orsolini, Norwegian Institute for Air Research, N-2027 Kjeller, Norway.

D. R. Jackson, Met Office, FitzRoy Road, Exeter EX1 3PB, UK. (david.jackson@metoffice.gov.uk)